

# Ballistic Lunar Transfers to Near Rectilinear Halo Orbit: Operational Considerations

Nathan L. Parrish<sup>1</sup>, Ethan Kayser<sup>2</sup>, Matthew Bolliger<sup>3</sup>,  
Michael R. Thompson<sup>4</sup>, Jeffrey S. Parker<sup>5</sup>, Bradley W. Cheetham<sup>6</sup>  
*Advanced Space LLC, 2100 Central Ave, Boulder, CO 80301*

Diane C. Davis<sup>7</sup>  
*ai solutions, 2224 Bay Area Blvd #415, Houston, TX 77058*

Daniel J. Sweeney<sup>8</sup>  
*NASA JSC, 2101 E. NASA Pkwy, Houston, TX 77058*

This paper presents a study of ballistic lunar transfer (BLT) trajectories from Earth launch to insertion into a near rectilinear halo orbit (NRHO). BLTs have favorable properties for uncrewed launches to orbits in the vicinity of the Moon, such as dramatically reduced spacecraft  $\Delta V$  requirements. Results are described from a detailed set of related mission design studies: BLTs with and without an outbound lunar flyby, insertion and rendezvous of a single spacecraft with a target in an NRHO, and insertion and rendezvous of multiple spacecraft with a target NRHO in quick succession. Monte Carlo analyses are presented of simulated rendezvous operations with realistic errors. These analyses are presented to inform future missions to NRHOs.

## I. Introduction

### A. Motivation

The Gateway is proposed as the next human outpost in space; a proving ground near the Moon for deep space technologies and a staging location for missions beyond Earth orbit and to the lunar surface. As the Gateway is constructed over time, both crewed and uncrewed payloads will frequently travel to the spacecraft. Examples include elements of the Gateway itself as the spacecraft grows in size, logistics modules carrying supplies, Human Lander System (HLS) elements to support a crewed lunar landing, and the Orion crew vehicle. Minimizing the cost of transfer from Earth to the Gateway enables successful construction, operations, and exploration.

The Gateway is planned to orbit the Moon in a Near Rectilinear Halo Orbit (NRHO), a nearly stable member of the  $L_2$  Halo family of orbits. The NRHO proposed for the primary Gateway orbit is characterized by a perilune radius of approximately 3,500 km and an apolune radius of about 71,000 km over the lunar south pole. With an orbital period of about 6.5 days, the southern  $L_2$  NRHO exhibits a 9:2 resonance with the lunar synodic period. A low-energy orbit, the NRHO sits at the top of the lunar gravity well, and thus, insertion into orbit is much less expensive than for a low lunar orbit. Nevertheless, fast transfers from the Earth to NRHO require significant  $\Delta V$ .<sup>9</sup> For uncrewed spacecraft without strict constraints on flight time, significant propellant savings can be achieved by allowing longer times of flight and employing the effects of solar gravity to naturally raise the orbit to the Moon. Such transfers are known as Ballistic Lunar Transfers (BLTs). Many previous investigations have explored the use of BLTs for transfer to various multibody orbits, both unstable and stable. BLTs have successfully been employed for transfer of several spacecraft

---

<sup>1</sup> Optimization Lead, Advanced Space, LLC, 2100 Central Ave STE 102, Boulder, CO 80301. AIAA member.

<sup>2</sup> Aerospace Engineer, Advanced Space, LLC, 2100 Central Ave STE 102, Boulder, CO 80301. AIAA member.

<sup>3</sup> Aerospace Engineer, Advanced Space, LLC, 2100 Central Ave STE 102, Boulder, CO 80301. AIAA member.

<sup>4</sup> Aerospace Engineer, Advanced Space, LLC, 2100 Central Ave STE 102, Boulder, CO 80301. AIAA member.

<sup>5</sup> Chief Technical Officer, Advanced Space, LLC, 2100 Central Ave STE 102, Boulder, CO 80301. AIAA member.

<sup>6</sup> Chief Executive Officer, Advanced Space, LLC, 2100 Central Ave STE 102, Boulder, CO 80301. AIAA member.

<sup>7</sup> Principal Systems Engineer, ai solutions, 2224 Bay Area Blvd #415, Houston TX 77058.

<sup>8</sup> Gateway Integrated Spacecraft Performance Lead, NASA Johnson Space Center, 2101 E. NASA Pkwy, Houston, TX 77058.

<sup>9</sup> J. Williams, D. E. Lee, R. L. Whitley, K. A. Bokelmann, D. C. Davis, and C. F. Berry, "Targeting Cislunar Near Rectilinear Halo Orbits for Human Space Exploration," 27th AAS/AIAA Space Flight Mechanics Meeting, Feb. 2017.

to lunar orbits, including the Hiten<sup>10</sup> and GRAIL<sup>11</sup> missions. A previous study<sup>12</sup> surveyed the use of BLTs for transfer to the Gateway NRHO. The current investigation explores operational considerations for BLTs to the NRHO. First, launch opportunities are investigated that allow near-simultaneous arrival of multiple spacecraft launched in subsequent months. Then, the sensitivities of the BLT trajectories to launch and maneuver execution errors are assessed, and a schedule of Trajectory Correction Maneuvers (TCMs) is proposed. Finally, orbit determination and tracking schedules are considered for BLTs to the NRHO.

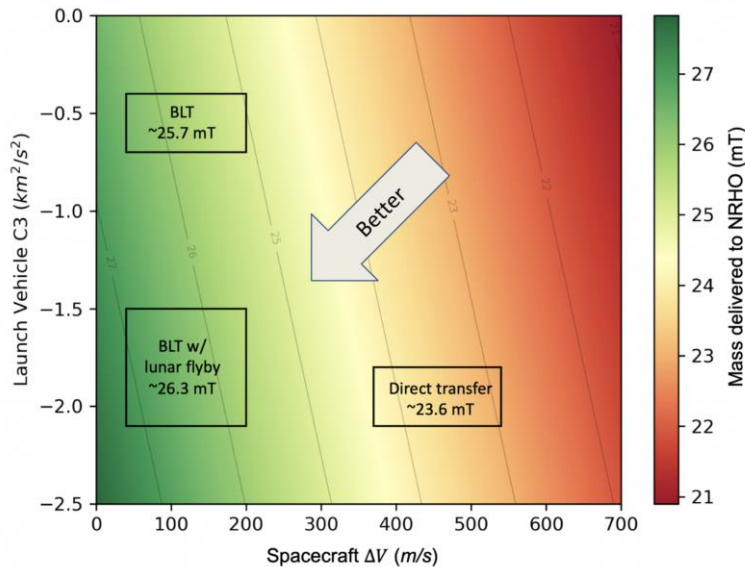


**Figure 1. Delivered dry mass for SLS Block 1.**

## B. Background

Ballistic lunar transfers (BLTs) exist for a variety of 3-body orbits.<sup>13</sup> In these transfer orbits, the Sun’s gravity is used to raise perigee and adjust inclination. In order for the Sun’s gravity to have a significant effect on the trajectory, the apogee must be approximately 1-2 million kilometers. A true “ballistic” transfer has no deterministic maneuvers required after launch, asymptotically approaching the target 3-body orbit along its unstable manifold or, in some cases, along a trajectory that harnesses perturbations without an unstable manifold.<sup>14</sup>

In the literature, studies of BLTs in the Sun-Earth circular restricted three body problem (CRTBP) have found many families of solutions which do not have a lunar flyby, and even more families of solutions which do have a lunar flyby<sup>15,16</sup>. Some of these families exist so close to each other that they are equivalent in terms of practical implementation. Two families of solutions with a lunar flyby are shown in Fig. 2. Two families of solutions without a lunar flyby are shown in Fig. 3.

<sup>10</sup> W.S. Koon, M. W. Lo, J. E. Marsden, and S. D. Ross, “Low Energy Transfer to the Moon,” *Celestial Mechanics and Dynamical Astronomy*, vol. 81, pp. 63-73, 2001.

<sup>11</sup> M. J. Chung, S. J. Hatch, J. A. Kangas, S. M. Long, R. B. Roncoli, and T. H. Sweetser, “Trans-Lunar Cruise Trajectory Design of GRAIL Mission,” AIAA/AAS Astrodynamics Specialists Conference, Toronto, Canada, August 2010.

<sup>12</sup> N. L. Parrish, E. Kayser, S. Udupa, J. S. Parker, B. W. Cheetham, and D. C. Davis, “Survey of Ballistic Lunar Transfers to Near Rectilinear Halo Orbit,” AAS/AIAA Astrodynamics Specialists Conference, Portland, Maine, August 2019.

<sup>13</sup> J. S. Parker and R. L. Anderson, *Low-Energy Lunar Trajectory Design*, DESCANSO Deep Space Communication and Navigation Series, John Wiley and Sons, Hoboken, New Jersey, June 2014.

<sup>14</sup> J. S. Parker, C. Bezrouk, and K. E. Davis, “Low-Energy Transfers to Distant Retrograde Orbits,” Proceedings of the AAS/AIAA Space Flight Mechanics Meeting, Paper AAS 15-311, Williamsburg, Virginia, 11-15 January 2015.

<sup>15</sup> Parker J. S. and Anderson R. L., “Low Energy Lunar Trajectory Design”, Elsevier 2013.

<sup>16</sup> Parker J.S., “Families of Low-Energy Lunar Halo Transfers”, *Advances in the Astronautical Sciences*, 2006.

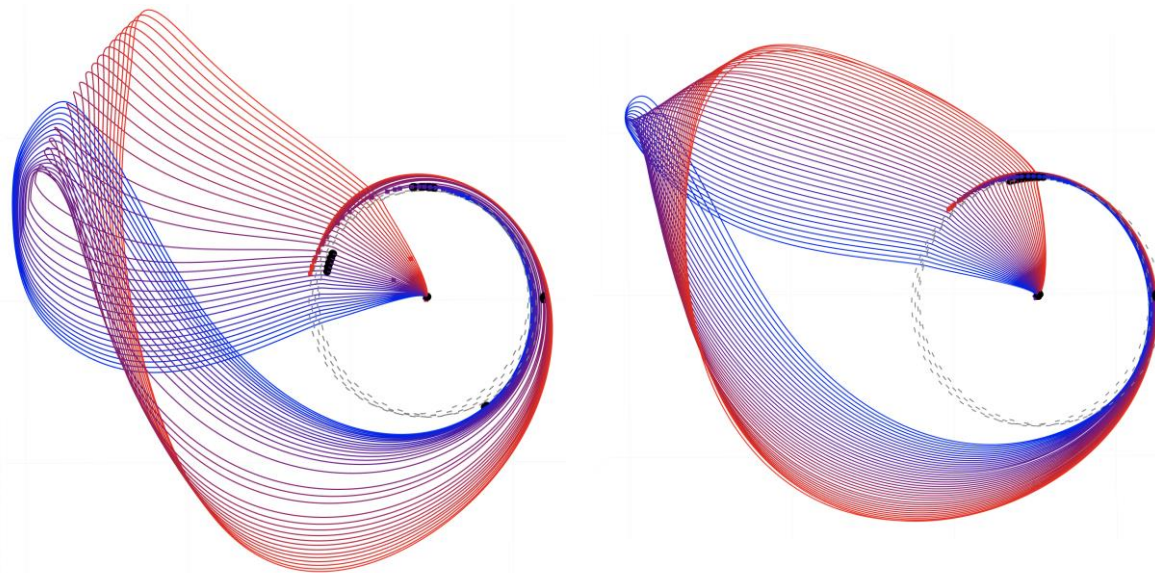


**Figure 2. Example BLTs with outbound lunar flyby. Each family is evaluated for several days to show the evolution of the family over time.**

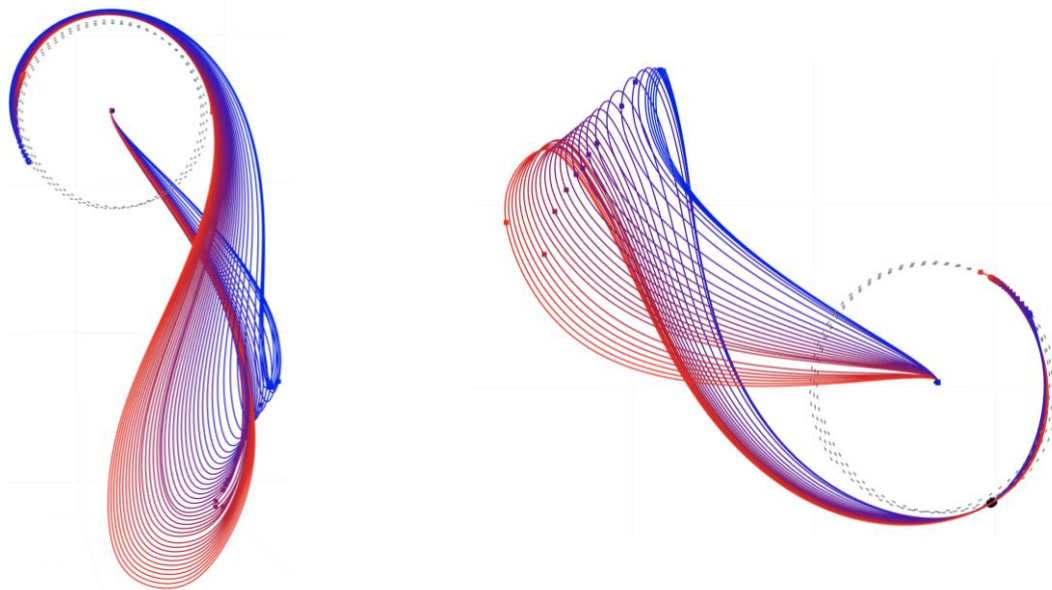


**Figure 3. Example BLTs without a lunar flyby. Each family is evaluated over one month to show the evolution of the family over time.**

## II. Dynamics and Assumptions

Spacecraft dynamics are modeled in multiple high-fidelity, verified NASA tools: GMAT (the General Mission Analysis Tool, developed at Goddard Space Flight Center)<sup>17</sup>, Monte (Mission Analysis, Operations, and Navigation Toolkit Environment, developed at the Jet Propulsion Laboratory)<sup>18</sup>, and Copernicus trajectory design and

<sup>17</sup> Jah, M., Hughes, S., Wilkins, M., and Kelecy, T. The General Mission Analysis Tool (GMAT): A New Resource for Supporting Debris Orbit Determination, Tracking and Analysis. 2009.

<sup>18</sup> Jonathon Smith, W. "MONTE Python for Deep Space Navigation." *Proceedings of the 15th Python in Science Conference*, No. Scipy, 2016, pp. 62–68. doi:10.25080/majora-629e541a-009.

optimization system<sup>19</sup>. In this analysis, GMAT or Copernicus generates the “truth” solution with the following forces modeled:

- 32x32 spherical harmonics gravity field model of the Moon from the GRGM 900c model.
- Point masses of the Earth, Sun, and barycenters of all other planetary systems in the solar system, with states from the JPL DE430 ephemerides<sup>20</sup>.
- Solar radiation pressure, with a cannonball model and assuming mass of 14,000 kg, surface area of 23 m<sup>2</sup>, and coefficient of reflectivity of 1.3. These are chosen to be representative of the Logistics Module for the Gateway.
- Relativistic correction.

The filter dynamics are slightly different from the “true” dynamics in order to represent realistic mis-modeling of small forces. The filter dynamics are implemented separately in GMAT and Monte and include the following forces:

- 8x8 spherical harmonics gravity field model of the Moon from the GRGM 900c model.
- Point masses of the Earth, Sun, and barycenters of all other planetary systems in the solar system, with states and GMs from the JPL DE430 ephemerides<sup>21</sup>.
- Solar radiation pressure with a spherical spacecraft. Mass, surface area, and coefficient of reflectivity are initialized randomly with error according to the uncertainties given in Table 2.
- No relativistic correction.

Navigation is simulated separately in GMAT and in Monte. In both navigation simulations, the filter defines the dynamics in an Earth-centered J2000 inertial reference frame.

The GMAT simulation uses a batch filter iterated until convergence. Convergence is defined as meeting the absolute and relative weighted RMS convergence criteria (0.01 and 0.001, respectively) and usually takes 3-5 iterations. GMAT’s outer loop sigma editing (OLSE) is not used here because the simulated measurements are known to all be valid. In real operations, outlier measurements would be ignored to avoid incorporating bad data into the filter solution.

The Monte simulation compares two different filters: the U-D factorized covariance filter, and the square root information filter (SRIF). The Monte filter uses stochastic accelerations on the order of  $5 \times 10^{-7}$  mm/s<sup>2</sup> updated every 8 hours to absorb dynamical mis-modeling.

In this analysis, a data arc is defined between maneuvers such as trans-lunar injection (TLI), trajectory correction maneuvers (TCMs), NRHO insertion maneuver (NIM), and insertion correction maneuvers (ICMs). Each data arc starts immediately following the previous maneuver and ends at the data cutoff 24 hours before the next maneuver. Maneuvers are not estimated. Future analysis will model the maneuvers in the filter and also allow tracking passes during the 24 hours between data cutoff and the next maneuver (these data would be used to estimate the state for the subsequent data cutoff).

All analyses in this paper use three DSN (deep space network) ground stations, with a maximum of one ground station active at a time. The ground stations simulate a 35-m dish at the Madrid, Canberra, and Goldstone facilities. The Gateway is assumed to communicate with the DSN on X-band radio. Measurement noise in reality is dependent on many factors, such as the ground radio specifications, spacecraft radio specifications, and weather in Earth’s ionosphere. The measurement noise specified in Table 1 is chosen to be similar to the real measurement noise found from post-processing of navigation data from the ARTEMIS mission<sup>22</sup>.

All maneuvers are assumed to be impulsive changes in velocity ( $\Delta V$ ). Launch is not modeled. The simulation begins in a 100 km circular parking orbit around Earth with inclination of 28.5°, approximating the condition immediately after launch from Kennedy Space Center.

**Table 1. Assumed sources of uncertainty.**

<i>Error source</i>	<i>Uncertainty (3<math>\sigma</math>)</i>
---------------------	---

<sup>19</sup> Ocampo, C. A. An Architecture for a Generalized Trajectory Design and Optimization System. in *International Conference on Libration Points and Missions* (2002).

<sup>20</sup> Folkner, W. M., Williams, J. G., Boggs, D. H., Park, R. S. & Kuchynka, P. *The Planetary and Lunar Ephemerides DE430 and DE431. Interplanet. Netw. Prog. Rep* 196, (2014).

<sup>21</sup> Folkner, W. M., Williams, J. G., Boggs, D. H., Park, R. S. & Kuchynka, P. *The Planetary and Lunar Ephemerides DE430 and DE431. Interplanet. Netw. Prog. Rep* 196, (2014).

<sup>22</sup> Leonard, J. M., Cheetham, B. W., and Born, G. H. Preliminary Evaluation of Earth-Moon Libration Point Orbit Navigation with Post-Processed ARTEMIS Data. 2014.

Mass uncertainty	3%
SRP area	30%
Coefficient of reflectivity	45%
OMM execution error	1.42 mm/s fixed, 1.5% proportional, 1 deg pointing
Measurement bias	7.5 m (range), 2.5 mm/s (range-rate)
Measurement noise	3 m (range), 1 mm/s (range-rate)

**Table 2. A priori state error and covariance.**

<i>Estimated parameter</i>	<i>3<math>\sigma</math> a priori state error relative to truth (applied once at start of simulation)</i>	<i>a priori covariance (re-initialized at the start of every data arc)</i>
Position in Earth-centered J2000	10 km	$\infty$ km
Velocity in Earth-centered J2000	10 cm/s	$\infty$ m/s
Coefficient of reflectivity	45%	$\infty$
Range measurement bias	1 m	$\infty$
Range-rate measurement bias	0.35 mm/s	$\infty$

### III. “Trifecta” BLT Launch Opportunities

A previous BLT mission design analysis studied over 70,000 optimal BLTs with outbound lunar flyby, with each BLT belonging to one of several distinct families<sup>23</sup>. The time of flight for these transfers varies from 16 to 25 weeks, which creates a unique opportunity: a “trifecta” of launches, spaced one month apart, which all rendezvous with the Gateway in the NRHO at the same time or within one week. Such a trio of transfers is beneficial for lunar human lander system architectures because the transfer vehicle, descent stage, and ascent stage can each launch separately and arrive at the Gateway together. An example is shown in Figure 4.

<sup>23</sup> N. L. Parrish, E. Kayser, S. Udupa, J. S. Parker, B. W. Cheetham, and D. C. Davis, “Survey of Ballistic Lunar Transfers to Near Rectilinear Halo Orbit,” AAS/AIAA Astrodynamics Specialists Conference, Portland, Maine, August 2019.

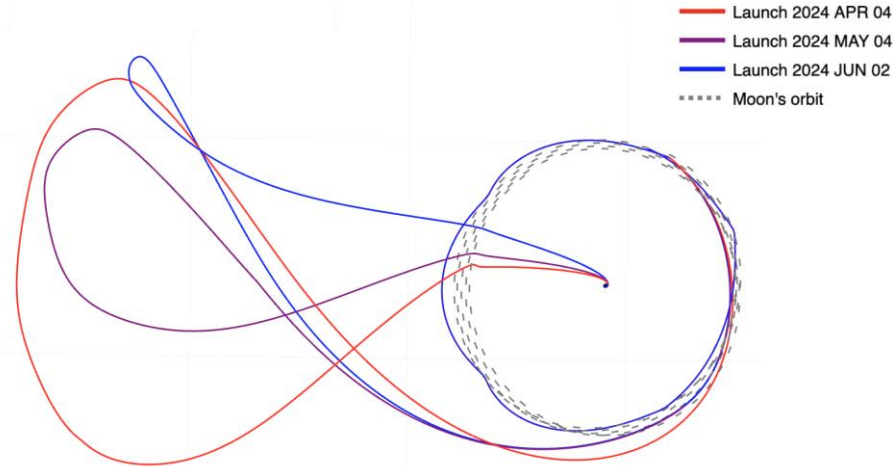


**Figure 4. Example of a “trifecta” set of BLTs.**

The launch period for each of these BLTs is found to vary greatly depending on the particular geometry constraints of a given launch. Some families of BLTs typically have launch periods as short as 1 day, while other families commonly have launch periods on the order of 10 days long. The launch periods can be extended by combining multiple families of solutions that exist near each other in the state space. If one of the three launches missed its launch period, it would have to arrive on a different NRHO revolution and would typically be delayed by approximately 1-3 weeks. Figure 5 shows the frequency at which these synchronized launch opportunities exist.

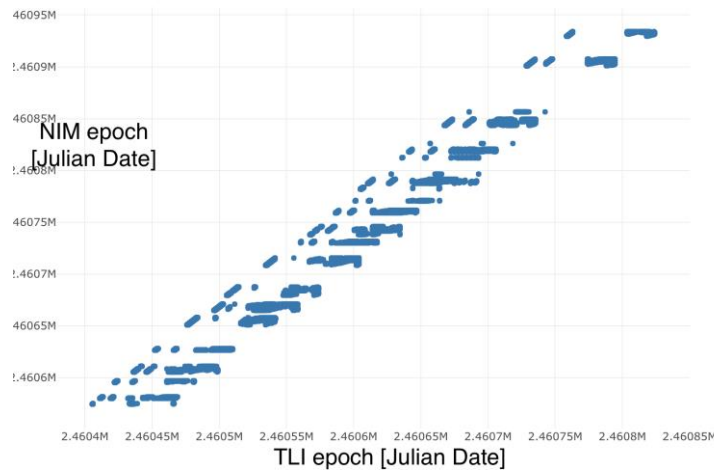


**Figure 5. Opportunities for multiple launches with synchronized arrivals.**

#### IV. Launch Injection Error

Three example nominal BLTs within the same launch period are used to study the effect of various sources of error on the  $\Delta V$  required to actually fly such a transfer. These BLTs do not include a lunar flyby, and represent the open, middle and close of a 10-day, representative launch period. Key parameters of these transfers are described in Table 4.

**Table 4. Nominal ballistic lunar transfer, without lunar flyby.**

	Launch Period		
	Open	Middle	Close

Deterministic TCM-2 $\Delta V$	25.4 m/s	1.6 m/s	25.2 m/s
Nominal Insertion $\Delta V$	15.8 m/s	15.8 m/s	15.9 m/s
Nominal Total $\Delta V$	41.2 m/s	17.4 m/s	41.1 m/s
TLI Epoch	April 4, 2024 12:00:00 UTC	April 9, 2024 12:00:00 UTC	April 14, 2024 12:00:00 UTC
Time of flight	111.6 days	106.6 days	101.3 days

The transfer is assumed to have 5 TCM's, located notionally at each of the stars in Figure 6. Additional details on the timing and targets of each TCM are given in Table 5.

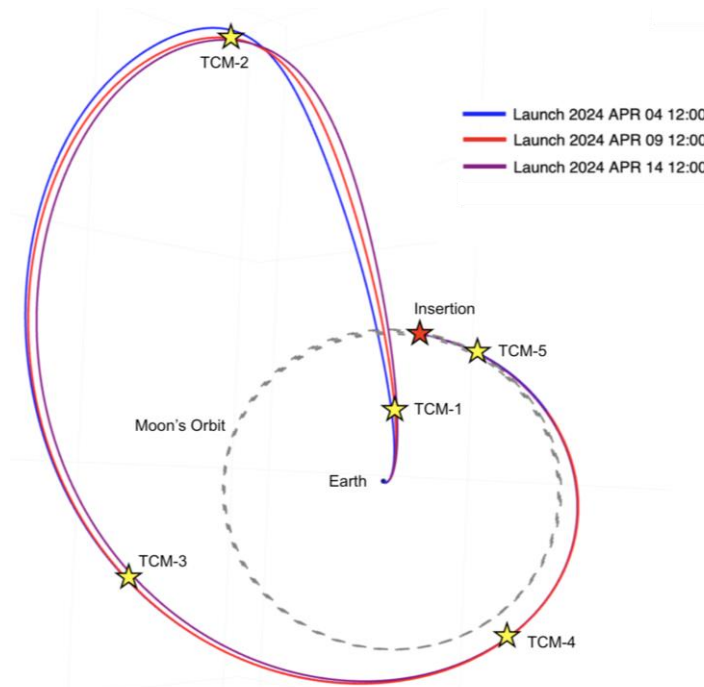


**Figure 6. Approximate locations of each TCM for the example BLT studied, showing the open, middle, and close of the launch period. Plotted in the J2000 inertial reference frame.**

**Table 5. Description of Trajectory Correction Maneuver (TCM) timing and design.**

<i>Maneuver</i>	<i>Timing</i>	<i>Design</i>
TCM-1	1 day after launch	Target position from back propagated nominal NRHO insertion at time of TCM-2 Minimize TCM-1 + TCM-2 $\Delta V$
TCM-2	65 days before insertion (or optimized)	Target position from back propagated nominal NRHO insertion at time of TCM-3 Minimize TCM-2 + TCM-3 $\Delta V$

TCM-3	30 days before insertion	Target position from back propagated nominal NRHO insertion at time of TCM-4 Minimize TCM-3 + TCM-4 $\Delta V$
TCM-4	10 days before insertion	Target position from back propagated nominal NRHO insertion at time of TCM-5 Minimize TCM-4 + TCM-5 $\Delta V$
TCM-5	1 day before insertion	Target post-insertion maneuver state (start of NRHO) Minimize TCM-5 + Insertion $\Delta V$

The nominal transfer is nearly ballistic, with a deterministic TCM-2  $\Delta V$  of 1.6 m/s and a total deterministic  $\Delta V$  of 17.4 m/s. The following set of analyses examine various contributors to the statistical  $\Delta V$ , beginning with the launch injection state error. Typical launch errors (based approximately on various launch vehicles the authors are familiar with) are considered, with  $3\sigma$  C3 error of  $0.1 \text{ km}^2/\text{s}^2$  and  $3\sigma$  angle error of 1 degree. Here, the angle error is represented as an error in argument of perigee (AoP), right ascension of ascending node (RAAN), and inclination. Figure 7 shows the contribution of each of these sources of error to the total TCM  $\Delta V$ . The open, middle, and close of a notional launch period are shown. At the open and close of this launch period, the nominal  $\Delta V$  is approximately 30 m/s. It is clear that the most significant error source is the launch C3. The middle of the launch period has  $\Delta V$  between 1.6 m/s and 30 m/s. The open and close of the launch period have  $\Delta V$  between 30 m/s and 55 m/s. In this figure, TCM-1 takes place 24 hours after trans-lunar injection (TLI).

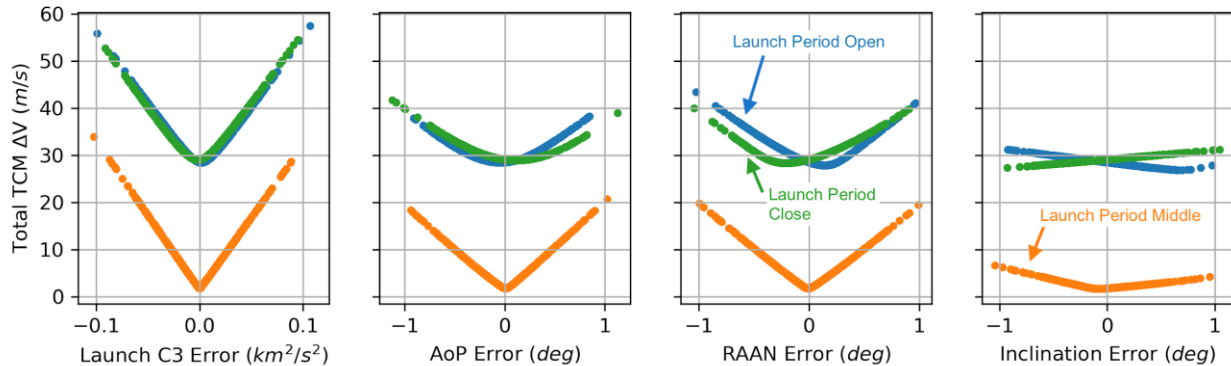


**Figure 7. Total TCM  $\Delta V$  as a function of launch error, with errors sampled individually.**

All sources of error (launch state, orbit determination, and maneuver execution) are then sampled together to understand the effect of their cross-coupling. This is shown in Figure 8, with TCM-1  $\Delta V$  as a function of launch C3 error and angle error, for the nominal launch epoch. In this figure, it is clear once more that the TCM error drives the TCM-1  $\Delta V$ . When the errors are considered together, the TCM-1  $\Delta V$  can exceed 50 m/s.

The timing of TCM-1 is considered between 12 hours and 96 hours after TLI. The earlier TCM-1 takes place, the lower the total  $\Delta V$  (errors can be corrected while still close to Earth). Practical navigation and operational constraints limit the time required between TLI and TCM-1.



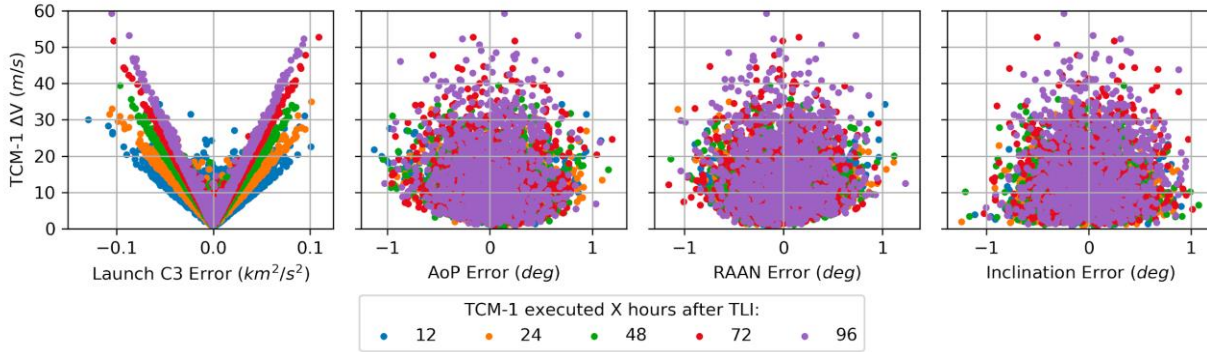


**Figure 8. TCM-1  $\Delta V$  as a function of launch error and TCM-1 timing, with errors sampled together.**

The launch vehicle injection error can, in some cases, be the largest contributor to the total spacecraft  $\Delta V$  requirements, so it is important to understand this effect.

## V. Navigation Requirements Analysis

The same nominal transfer from Section IV is used again here. Requirements on BLT navigation accuracy are considered by exploring the relationship between navigation uncertainty and TCM  $\Delta V$ , and by exploring the relationship between navigation uncertainty and NRHO insertion accuracy. A navigation requirements simulation is performed with the following errors modeled:

- Launch injection,
- Navigation error (found by randomly perturbing the truth according to an assumed distribution for navigation uncertainty), and
- Maneuver execution error (using the Gates model<sup>24</sup> with fixed and proportional pointing errors and fixed and proportional magnitude errors).

For each of the trades shown below, a Monte Carlo analysis of 1,000 trials each is performed. In each trial, the BLT is built up one maneuver at a time. Each TCM is designed according to the logic described in Table 5, above. Essentially, each TCM is considered as the first of two maneuvers to retarget the nominal transfer. In some trials, the NRHO insertion maneuver (NIM) is allowed to change during each TCM design, and in others, the NIM is held fixed until the TCM-5 design. TCM-5 and NIM are designed together, so the NIM design is fixed at the TCM-5 data cutoff epoch (two days before NIM execution).

A 24-hour data cutoff is enforced for each TCM. To simulate this, the specified navigation error is sampled at the data cutoff epoch. The sample (with error) is then propagated to the maneuver execution epoch and executed with random errors according to the Gates model. The TCM is designed based on the truth trajectory and executed by the sample with simulated OD error — which becomes the new truth trajectory going forward. TCM-1 occurs shortly after launch, so the data cutoff is reduced to 8 hours before the maneuver execution epoch in that case.

### *TCM placement trades.*

There is no obvious ideal number of TCMs or timing of TCMs. Some things are clear, though, from experience. For instance, it is clear from the analysis of the launch error and TCM-1 that TCM-1 should be performed as soon as it is feasible. TCM-2 (located nominally at apogee) is the only one designed to have a deterministic component. Using that deterministic maneuver to also clean up errors is beneficial because the vector addition of the deterministic and stochastic components will be less than or equal to the magnitude of the two components separately. Early analysis of BLTs found that the transfers are highly sensitive to the NRHO insertion state, so it is reasonable to add a clean up maneuver shortly before NRHO insertion — TCM-5 in this analysis.

The real question, then, is how many TCMs should take place between TCM-2 and the maneuver immediately before NRHO insertion. Preliminary results find that having two TCMs between these other maneuvers is preferable to having just one TCM in that segment of the trajectory. The number of TCMs thus comes out to 5, with the approximate timing discussed above in Table 5. The results of an analysis are shown below in Tables 7-9 to consider the optimal timing of TCM-3 relative to the NRHO insertion, for the open, middle, and close of the launch period. Each of these three tables shows the mean and 99th percentile  $\Delta V$  ( $\Delta V_{99}$ ) for each TCM individually and the total of

<sup>24</sup> Gates, C. R. *A Simplified Model of Midcourse Maneuver Execution Errors*. Pasadena, CA.

all TCMs. Each column in each table represents a Monte Carlo analysis of 500 random samples. For these results, the  $3\sigma$  navigation error was assumed to be 3/30/30 km and 3/30/30 cm/s (radial/transverse/normal directions), and the  $3\sigma$  maneuver execution error was assumed to be 3 cm/s fixed error and 3% proportional error in both magnitude and pointing. Later sections of this report consider the effect of changing the navigation and maneuver execution errors.

**Table 7. TCM-3 timing study, for beginning of launch period.**

$\mu/P99$ (m/s)	TCM-3 Execution Time (days before NIM)				
Maneuver	No TCM-3	20	30	40	50
TCM-1	11.20 / 27.67	11.65 / 27.50	11.31 / 28.03	11.54 / 29.99	11.53 / 29.87
TCM-2	25.33 / 27.92	25.33 / 27.54	25.39 / 28.04	25.39 / 27.62	25.43 / 27.95
TCM-3		9.04 / 27.44	3.70 / 12.25	1.77 / 5.67	1.02 / 3.01
TCM-4	25.13 / 80.09	2.04 / 7.82	0.96 / 3.69	1.22 / 3.41	1.95 / 5.76
TCM-5	25.64 / 84.75	5.08 / 16.45	5.47 / 15.07	5.70 / 15.39	5.945 / 15.44
<b>Total</b>	87.29 / 203.35	53.14 / 85.29	46.82 / 68.48	45.61 / 65.36	45.88 / 64.15

**Table 8. TCM-3 timing study, for middle of launch period.**

$\mu/P99$ (m/s)	TCM-3 Execution Time (days before NIM)				
Maneuver	No TCM-3	20	30	40	50
TCM-1	11.37 / 29.25	11.48 / 28.50	11.43 / 28.20	11.53 / 29.23	11.54 / 28.44
TCM-2	2.41 / 5.14	2.36 / 5.88	2.41 / 5.92	2.45 / 5.60	2.39 / 5.80
TCM-3		1.94 / 5.98	0.82 / 2.40	0.46 / 1.25	0.37 / 1.16
TCM-4	5.23 / 16.94	0.46 / 1.16	0.53 / 1.59	1.05 / 3.19	1.92 / 6.34
TCM-5	7.88 / 23.70	4.95 / 16.14	5.27 / 17.09	5.61 / 15.32	6.06 / 18.25
<b>Total</b>	26.89 / 57.21	21.19 / 42.84	20.47 / 41.79	21.10 / 43.54	22.27 / 45.01

**Table 9. TCM-3 timing study, for end of launch period.**

$\mu/P99$ (m/s)	TCM-3 Execution Time (days before NIM)				
Maneuver	No TCM-3	20	30	40	50
TCM-1	11.20 / 27.38	11.33 / 28.18	11.29 / 28.66	11.37 / 28.37	11.47 / 28.88
TCM-2	25.12 / 28.61	25.12 / 28.37	25.16 / 29.37	25.16 / 28.40	25.15 / 28.64
TCM-3		6.18 / 19.58	2.32 / 7.95	1.23 / 3.57	0.77 / 2.11
TCM-4	17.14 / 56.07	1.24 / 5.20	0.72 / 2.23	1.19 / 3.54	1.96 / 6.32
TCM-5	18.66 / 62.95	4.89 / 15.60	5.18 / 15.84	5.84 / 16.57	5.87 / 16.66

<b>Total</b>	72.12 / 154.28	48.76 / 73.95	44.66 / 64.91	44.77 / 63.76	45.23 / 67.31
--------------	----------------	---------------	---------------	---------------	---------------

From this analysis, the optimal timing of TCM-3 can be selected for each case. At the beginning of the launch period, the lowest  $\Delta V_{99}$  results from performing TCM-3 at 50 days before NIM. This is likely because TCM-2 has a significant deterministic cost ( $\Delta V_{99}$  of 28 m/s), so TCM-3 acts as a cleanup maneuver for TCM-2. In the middle of the launch period, the optimal timing of TCM-3 is at 30 days before NIM. In this case, TCM-2 is small ( $\Delta V_{99}$  of 6 m/s), so it is preferable to have TCM-3 later in the transfer so that it is more evenly spaced between TCM-2 and TCM-4. At the end of the launch period, the optimal timing (minimum total  $\Delta V_{99}$ ) of TCM-3 is at 40 days before NIM, similar to the beginning of the launch period.

*Effect of TCM-5 execution error on NRHO insertion error*

For this analysis, the NIM is assumed to be performed at perilune, at which point the orbital energy change can be accomplished for the minimum  $\Delta V$ . There is a trade-off between maneuver efficiency and the accuracy of the achieved insertion state. The closer NIM is performed to perilune, the smaller the maneuver can be because of the Oberth effect<sup>25</sup>. However, the Oberth effect also means that orbit determination errors and maneuver execution errors are magnified. The present study finds that given reasonable OD knowledge before NIM (so that TCM-5 and NIM can be designed accurately) and after NIM (so that cleanup maneuvers can be executed within the first revolution of the NRHO), executing NIM at perilune is the most fuel efficient option. Figure 9 shows the achieved NRHO insertion state error mapped to perilune, as a function of the TCM-5 maneuver execution error. The NRHO insertion state error is represented in the Moon-centered, Earth-Moon rotating frame, while the maneuver execution errors are represented in an Earth-centered inertial frame. Figure 10 shows the same insertion error as a function of the state error immediately after TCM-5, which is analogous to the orbit determination error. From these figures, the most significant contributor to the insertion error is the velocity state error after TCM-5. This suggests that reducing the OD uncertainty would be the most effective way to reduce the NRHO insertion error.

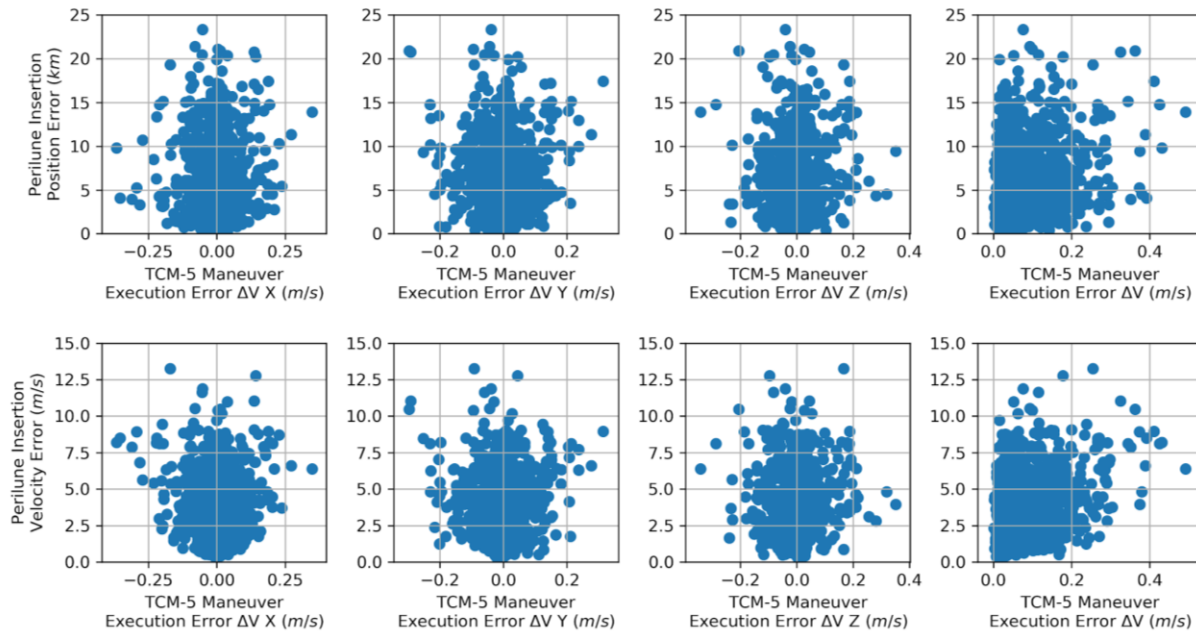


**Figure 9. TCM-5 execution error vs. NRHO insertion error.**

<sup>25</sup> Oberth, H. *Ways to Spaceflight*. R. Oldenbourg Publishing House, 1929.

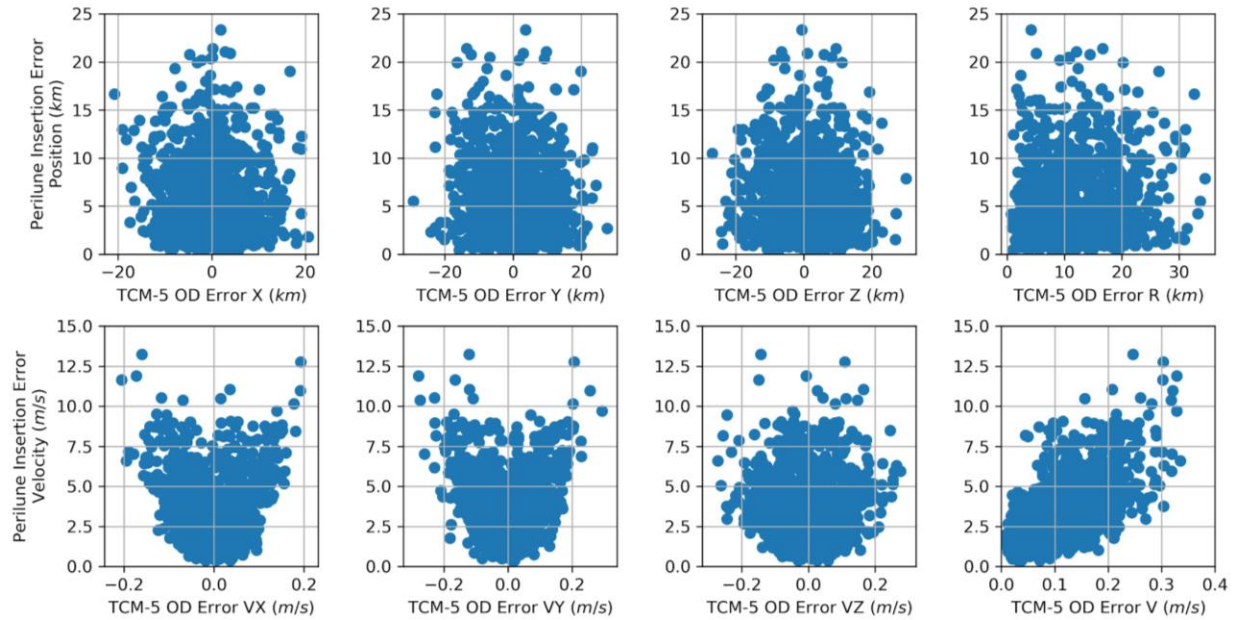


**Figure 10. State error immediately after TCM-5 vs. NRHO insertion accuracy.**

Since NRHO insertion is a very sensitive maneuver, there is a trade-off between deterministic  $\Delta V$  and stochastic  $\Delta V$ . The closer the insertion maneuver is to perilune, the stronger the Oberth effect, and the more efficient the nominal maneuver execution. However, the Oberth effect also multiplies errors from orbit determination or maneuver execution. A previous analysis found that the deterministic  $\Delta V$  for NRHO insertion can be 10-30 m/s lower when insertion is performed near perilune than when performed 24 hours later.<sup>26</sup> If the cleanup maneuver(s) require less  $\Delta V$  than the  $\Delta V$  savings from inserting at perilune, then it is better to choose to insert at perilune. A parallel study explores the insertion correction maneuver strategy and  $\Delta V$  requirements.<sup>27</sup>

#### **A. Effect of OD uncertainty on future TCMs, total $\Delta V$ , & insertion accuracy**

The next analysis considers the effect of assumed OD uncertainty on the  $\Delta V$  for each TCM, NIM, and the mission total, as well as the effect on the NRHO insertion state. Two cases are examined: one with a high assumed OD uncertainty, and one with a low assumed OD uncertainty. The high uncertainty case uses  $3\sigma$  OD errors of 3/30/30 km and 3/30/30 cm/s in the radial/transverse/normal (RTN) directions of a frame defined by the spacecraft motion relative to Earth. The low uncertainty case uses  $3\sigma$  OD errors of 0.3/3/3 km and 0.3/3/3 cm/s in the RTN frame. A Monte Carlo analysis was run with 1,000 samples each for the high- and low-error cases. Figures 11 and 12 show the transfer  $\Delta V$  requirements for the high- and low-error cases, respectively, broken down by the  $\Delta V$  for each maneuver and the total  $\Delta V$ .

<sup>26</sup> N. L. Parrish, E. Kayser, S. Udupa, J. S. Parker, B. W. Cheetham, and D. C. Davis, "Survey of Ballistic Lunar Transfers to Near Rectilinear Halo Orbit," AAS/AIAA Astrodynamics Specialists Conference, Portland, Maine, August 2019.

<sup>27</sup> Parrish, N. L., Kayser, E., Bolliger, M., Thompson, M.R., Parker, J.S., Cheetham, B.W., Davis, D.C., "Near Rectilinear Halo Orbit Determination with Simulated DSN Observations", in *AIAA/AAS Spaceflight Mechanics Conference*, Orlando, 2020.

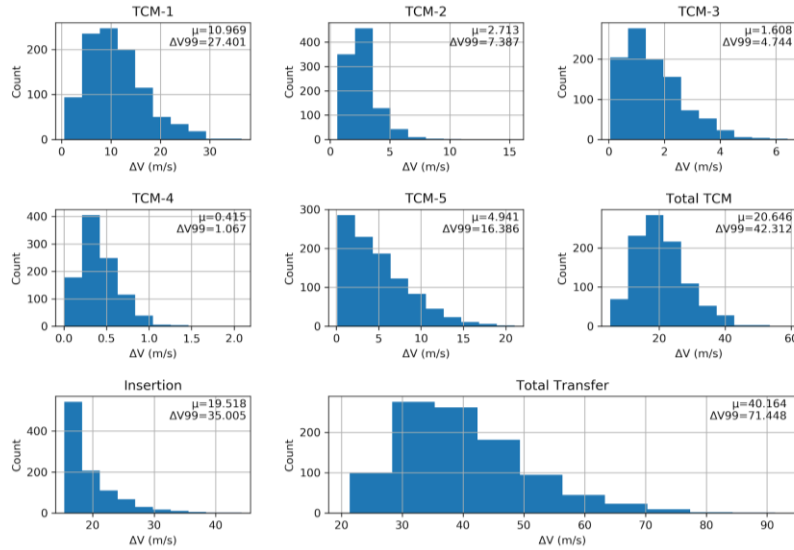


Figure 11. BLT transfer  $\Delta V$  requirements, with  $3\sigma$  orbit determination errors of 3/30/30 km, 3/30/30 cm/s in RTN frame.

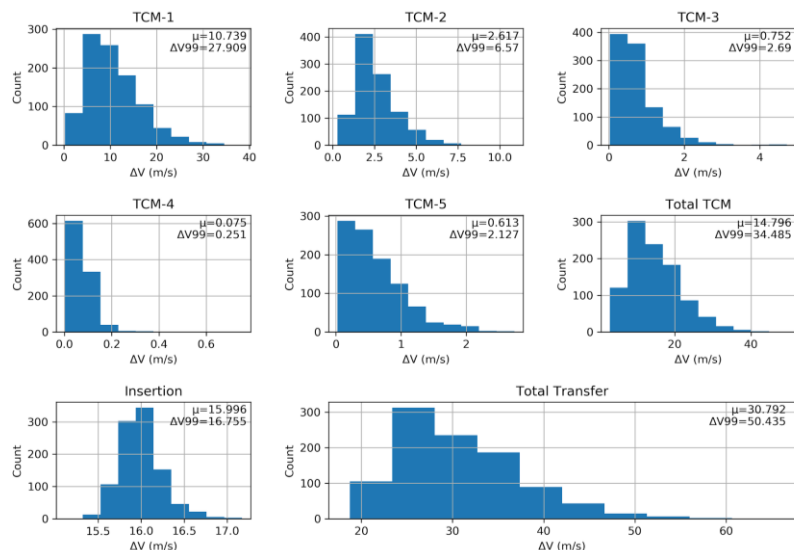
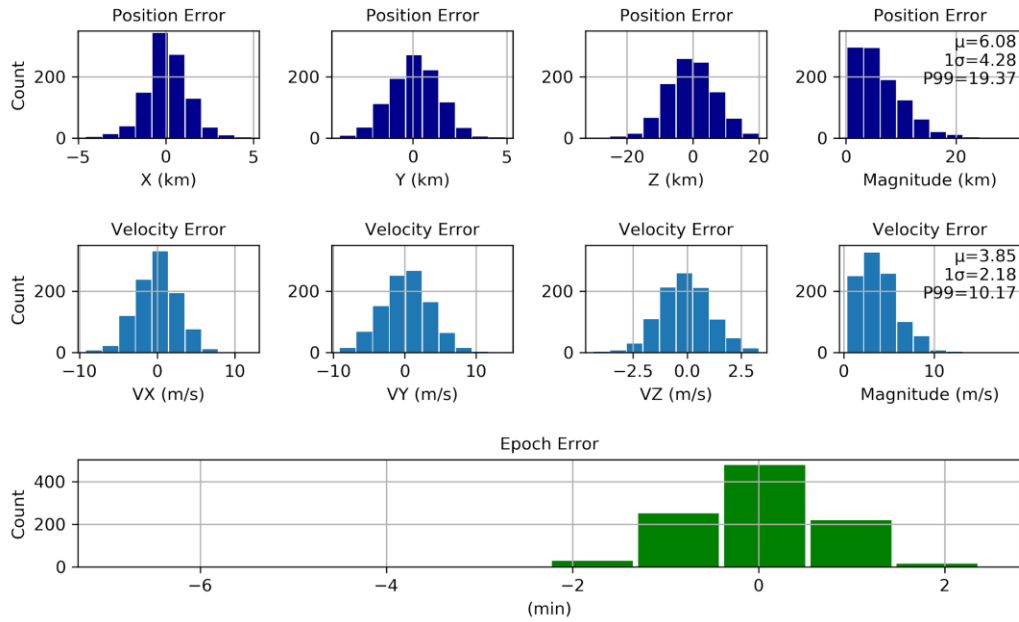


Figure 12. BLT transfer  $\Delta V$  requirements, with  $3\sigma$  orbit determination errors of 0.3/3/3 km, 0.3/3/3 cm/s in RTN frame.

As a result of the different geometry for each maneuver relative to the Earth, Moon, and Sun, some maneuvers are more sensitive than others. TCM-1 is 27-28 m/s regardless of the OD error because TCM-1 is mainly determined by the launch error. For this transfer, TCM-2 is small ( $\Delta V_{99}$  of approximately 7 m/s) regardless of the OD error, as the main contributor to TCM-2  $\Delta V$  is TCM-1 execution error. TCM-5 is different in that it varies substantially as a function of OD error — the high error case has a  $\Delta V_{99}$  of 16 m/s, and the low error case has a  $\Delta V_{99}$  of 2 m/s. This insight is useful because it informs where additional ground station tracking is most beneficial. The total transfer  $\Delta V_{99}$  is 71 m/s for the high error case and 50 m/s for the low error case.

Figure 13 shows the NRHO insertion error mapped to perilune for the large assumed OD uncertainty, and Figure 14 shows the same error for the small assumed OD uncertainty. Reducing the assumed OD uncertainty by a factor of 10 produced nearly the same amount of reduction in the achieved insertion state, confirming that the OD error is indeed the primary contributor to the insertion accuracy. Given that the NRHO is sensitive enough that a 15-20 m/s maneuver is sufficient to insert or depart the NRHO within a single revolution, the up-to 10 m/s achieved velocity error for the large OD error case is not acceptable. The tracking schedule must be chosen such that something similar to the small assumed OD error is achieved for the state estimate prior to TCM-5.



**Figure 13. Perilune insertion state error in Earth-Moon rotating frame with  $3\sigma$  orbit determination errors of 3/30/30 km, 3/30/30 cm/s in RTN frame.**

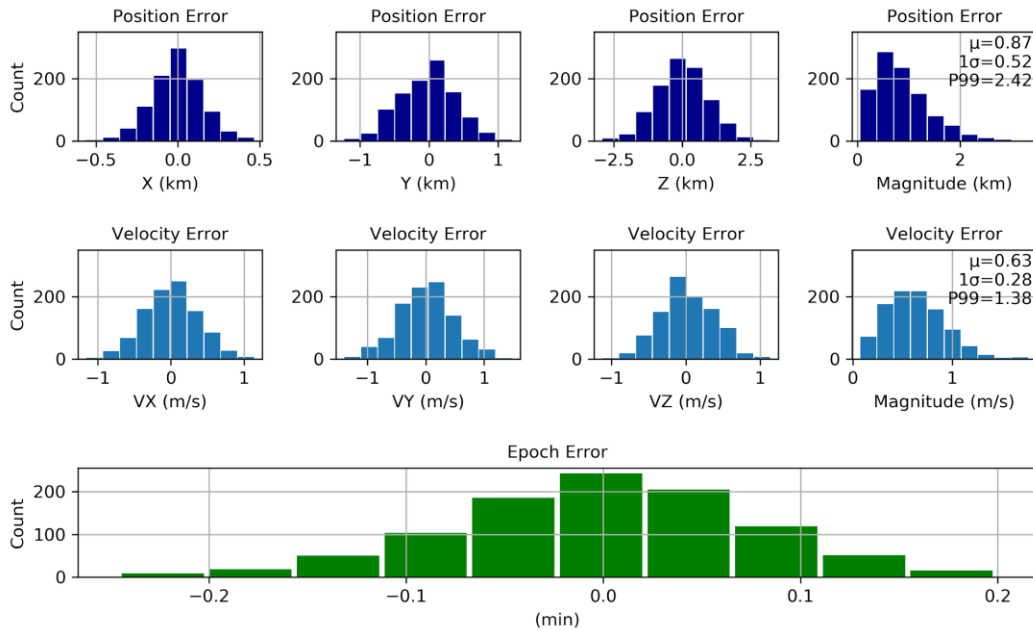


**Figure 14. Perilune insertion state error in Earth-Moon rotating frame with  $3\sigma$  orbit determination errors of 0.3/3/3 km, 0.3/3/3 cm/s in RTN frame.**

Figure 15 shows the relationship between the OD errors at one TCM and the  $\Delta V$  required at the next TCM. It is clear that the velocity component of the OD uncertainty is a large driver for the subsequent TCM's  $\Delta V$ . This analysis also suggests a way to reduce the statistical  $\Delta V$  for a transfer: strategic use of ground tracking to reduce the OD error at key points. For instance, adding extra tracking passes (and thus, reducing the state error) before TCM-4 could reduce the  $\Delta V$  for TCM-5 by as much as 18 m/s.

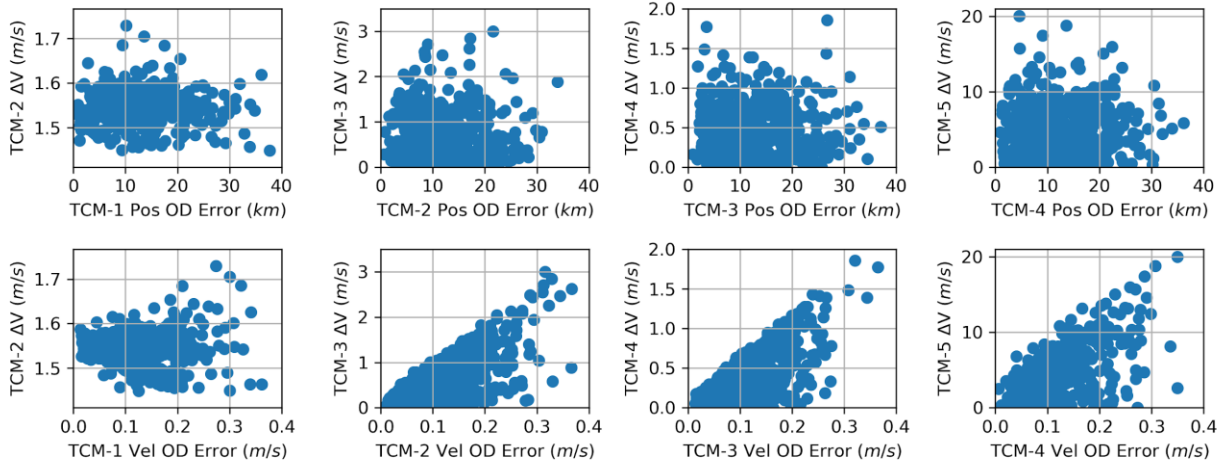


Figure 15. Relationship between OD error at each TCM and the  $\Delta V$  to recover at the next TCM.

## VI. BLT Navigation with Simulated Orbit Determination

Simulated orbit determination is performed in Monte using the U-D factorized covariance filter. The dynamics for the truth and navigation spacecraft as well as the assumptions about DSN noise are described in Section II. To mimic operational realism, the truth spacecraft is propagated outside of Monte entirely. The simulated measurements are generated in Monte, but the filter never comes into contact with the raw truth states. For this analysis, the following tracking cadences are evaluated:

- Continuous
- 8 hours per pass, 7 passes per week
- 8 hours per pass, 3 passes per week
- 8 hours per pass, 2 passes per week
- 2 hours per pass, 7 passes per week
- 2 hours per pass, 3 passes per week
- 2 hours per pass, 2 passes per week

The state uncertainties at each TCM are calculated for each of the proposed tracking schedules. For each tracking leg, the a priori state estimate is taken as the previous leg's final state perturbed by the 3-sigma covariance.

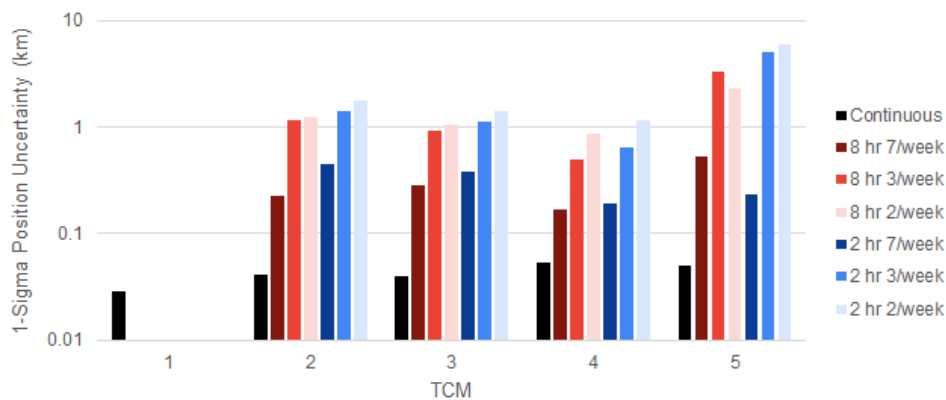
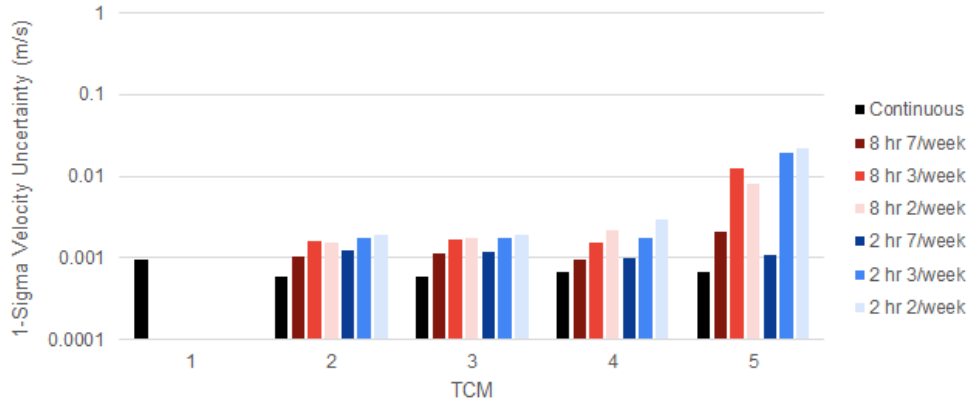


Figure 16. Position 1-sigma uncertainty at each TCM for various tracking cadences.



**Figure 17. Velocity 1-sigma uncertainty at each TCM for various tracking cadences.**

It is worth noting, particularly for the leg between TCM-4 and TCM-5 that the timing of the placement of the tracking passes seems to be more impactful on the final covariance than the length, or even cadence of passes. For example, see that the position and velocity uncertainty for the 8 hours per pass / 2 times per week is less than the 8 hours per pass / 3 times per week case. This is likely due to the fact that the TCM-4 to TCM-5 leg is only 8 days long, and as a result, the time between the final tracking pass and the end of the leg can have a large impact on the uncertainty at the end of the leg.

Figure 18 illustrates an important trend: the way the instantaneous position and velocity uncertainty grows between tracking passes and shrinks quickly during each tracking pass. In this example, there is an 8-hour pass twice per week for the entire transfer. The TCMs for this BLT are small, so the filter is able to build them into the dynamics purely with stochastic acceleration. A more accurate solution could be found by also estimating the maneuvers with the filter.

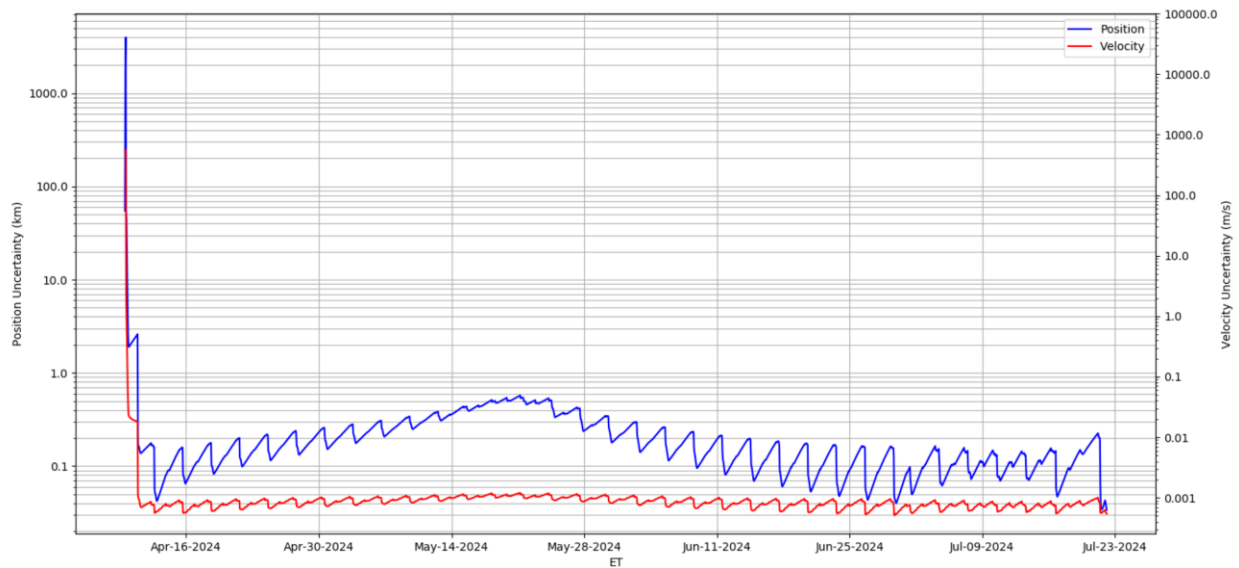


**Figure 18. Position and velocity 1-sigma uncertainty over an entire BLT. TCMs are modeled purely by stochastic acceleration in the filter.**

In order to verify the accuracy of the covariance estimate, a Monte Carlo analysis is run with simulated measurements. For each of the transfer legs, 100 random samples of simulated navigation are performed. Each sample uses different simulated measurements with the same tracking schedule. The standard deviation of the state estimates from running the filter is shown for each case in Figures 19-20.



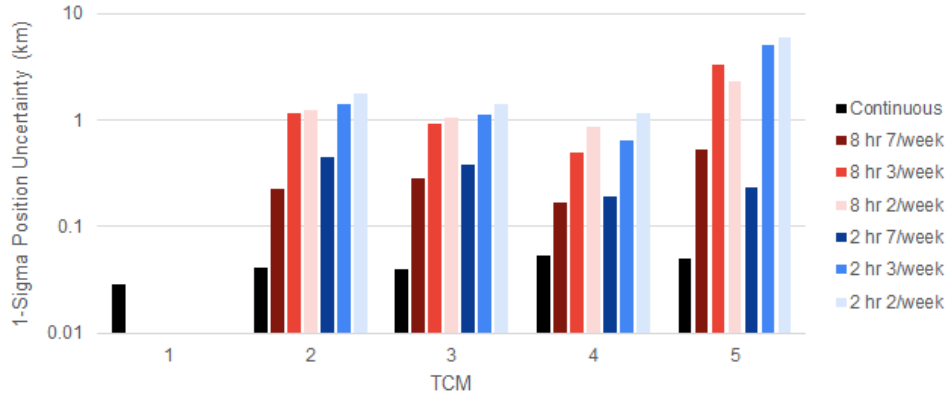


Figure 19. Position standard deviation of state estimates at each TCM for various tracking cadences.

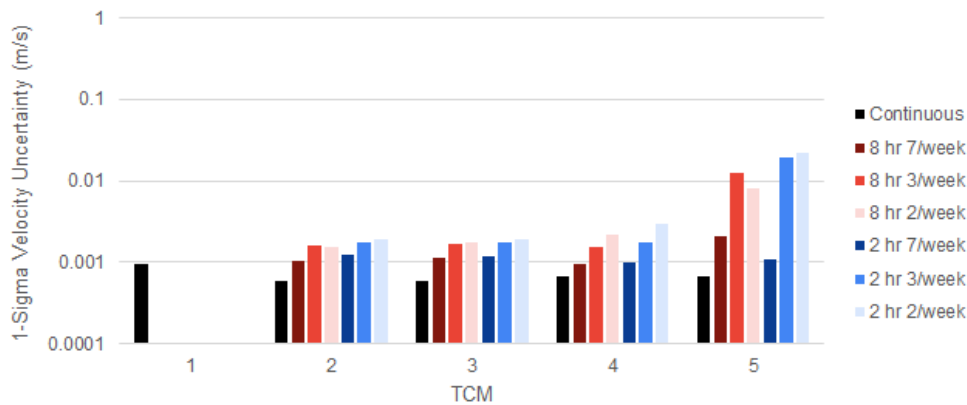


Figure 20. Velocity standard deviation of state estimates at each TCM for various tracking cadences.

The navigation requirements analysis resulted in the relationship between navigation accuracy, mission  $\Delta V$ , and NRHO insertion accuracy. The simulated OD study resulted in the relationship between tracking cadence and navigation accuracy. Given these two relationships, it is now possible to infer the relationship between tracking cadence and mission  $dV$  and between tracking cadence and NRHO insertion accuracy. It is assumed that there is continuous tracking for the 24 hours between launch and TCM-1, which is common because of the importance of correcting launch vehicle injection errors quickly. For each of the other TCMs, the analyses presented here can be used to prioritize when frequent tracking is most valuable.

## VII. Conclusion

The analyses in this paper address a range of questions related to navigating a spacecraft on a BLT to an NRHO. Realistic requirements for launch injection error, tracking cadence, tracking measurement noise, and tracking pass phasing are derived from analysis.

Future work will consider additional combinations of the various trades presented here. The sensitivity of the outbound lunar flyby will be studied in order to understand operational requirements for those families of transfers. NASA and Advanced Space will fly a low-energy transfer similar to the ones studied here (without an outbound lunar flyby) with the CAPSTONE mission, currently planned for launch in December 2020.

The authors wish to acknowledge support from the NASA SBIR (Small Business Innovative Research) program, and Caltech for the use of Monte software.